

## Cerebellum of Rats, As Affected by Zinc Oxide Nanoparticles and The Role of Selenium

Salma Samir Nassar<sup>\*1</sup>, Ali Mohamed Abd El-Gawad<sup>2</sup> and El-Sayed Nasr Salama<sup>3</sup>

1-3: Zoology Department, Faculty of Science, Zagazig University, Zagazig, Egypt

Corresponding author: Salma S. Nassar

E-mail: [nassarsalma52@gmail.com](mailto:nassarsalma52@gmail.com)

Conflict of interest: None declared

Funding: No funding sources

### Abstract

The progressive utility and application of zinc oxide nanoparticles (ZnO NPs) in medical and industrial purposes raises the debates about their safety use. Modern research recorded brain (CNS) as a target for NPs- toxicity. We sought to investigate the effects of selenium (Se) on ZnO NPs-neurotoxicity in rats. Forty adult male rats (*Rattus norvegicus*) weighing 180-200 g were randomly divided into four groups; control, Se-administered (0.2 mg/kg/day), ZnO NP-exposed (1 g/kg/day for 5 consecutive days), and ZnO NPs + Se, were used. Nanoparticles of ZnO appeared spherical with nearly uniform size and a mean diameter of 25.3 nm by transmission electron microscope (TEM). Exposure of rats to ZnO NPs recorded histopathological and ultrastructure lesions including; vacuolated molecular layer with apoptotic nerve cells, damaged and shrunken Purkinje cells (PC), swollen Bergman astrocytes and degenerated granular cells overlapped in gliosis. At EM level, PC appeared with ill-defined nuclear criteria and ruptured mitochondria, Bergmann astrocytes exhibited vacuolated cytoplasm with damaged mitochondria, granular cells had heterochromatic nuclei with irregular nuclear envelopes and vacuolated cytoplasm and molecular layer with dysmyelinated nerve fibers. The present results confirmed ZnO NPs-induced DNA injury in rat's cerebellum at the dose level of 1g/kg /day as recorded from comet data. However, administration of Se prior to ZnO NPs – exposure improved the histological, ultrastructural and molecular criteria of cerebellum. Conclusion: The study confirmed the neurotoxicity of ZnO NPs in rat's cerebellum and suggests a promising neuro-protective role of Se as a food supplement.

**Keywords:** Zinc oxid nanoparticles; Cerebellum of rats; Histopathology; Ultrastructure; Comet assay

**Tob Regul Sci.™ 2022;8(1): 1946-1964**

**DOI: [doi.org/10.18001/TRS.8.1.149](https://doi.org/10.18001/TRS.8.1.149)**

### Introduction:

Nanotechnology is a rapidly developing science and has been one of the fastest-growing technologies. Moreover, owing to their good antibacterial and antifungal properties, ZnO NPs are widely used in medicine. Previous investigators evaluated the toxicity of ZnO NPs in distinctive organs

(liver, renal tissues and testes) for short and long periods of exposure. They reported that ZnO NPs has the excessive potential to pass via placenta and blood organ barriers causing cellular and tissue damage (Zanchi *et al.*, 2015; Nassar *et al.*, 2017 ; Al-Salmi *et al.*, 2019). NPs are accumulated in brain tissue and induced oxidative stress resulting in neuro-degeneration. The latter disturbs CNS criteria and hence affects function of neurons (Ransohoff, 2016). Shim *et al.* (2014) recorded potential pathogenic effect of ZnO NPs in brain and blood and they bound to apolipoprotein, which acts as a mediator in NPs transportation across the BBB. Other studies revealed that ZnO NPs could induce apoptosis, cyto and genotoxicity, mitochondrial dysfunction and inflammatory responses (Yuan *et al.*, 2010; Sharma *et al.*, 2011). Hazardous effects of zinc oxide nanoparticles on different visceral organs such as kidney, liver, lung, spleen, and heart could be recorded (Jachak *et al.*, 2012; Li *et al.*, 2012). Moreover, DNA damage could be recorded in epidermal cells exposed to ZnO NPs for 6 h at different concentrations (Sharma *et al.*, 2009). Nanoparticles of zinc oxide induce intense DNA damage in bone marrow cellularity and blood as manifested by chromosomal fragmentation. These NPs suppressed the process of DNA repair via down regulating the immunoreactivity of proteins (Pati, 2016). Due to the progressive medical application of nanoparticles (particularly, metallic ones), more alertness was directed to the benignity of using them for the central nervous system (Sawicki *et al.*, 2019). The metal-rich nanoparticles are absorbed into circulation and deposited in different organs but the brain is the most susceptible one to their toxicity (Feng *et al.*, 2015).

Therefore, the objective of the present study is to evaluate the histological, ultrastructural and molecular effects of ZnO NPs on rat's cerebellum and the conceivable protective potential of selenium.

## MATERIAL AND TECHNIQS

### *Chemicals*

All chemicals used in the current study were products of Sigma (Sigma-Aldrich Corporation, USA) and being of high analytical grade. Zn O-NPs (MW: 81.39 g/mol, < 50 nm size, lucidity > 97% with prolonged action). Se was in the form of Sodium selenite (Na<sub>2</sub>SeO<sub>3</sub>).

### *Animals*

Animals used in the current experiment were bred in the special animal house of Faculty of Science, Zagazig University (40 adult male albino rat; *Rattus norvegicus*, 10-12 week). They were kept under standard conditions of dark / light cycle, temperature (25°C ±1), humidity (55%) and well-ventilated room. Water and food (standard pellets) were given *ad libitum*.

### *Animal grouping and dosage*

Animals were equally-divided into 4 groups; G1: Control, G2: Selenium group (orally-given 0.2 mg/kg/day) (El-Demerdasha and Nasr, 2014), G3: ZnO NPs group (orally-given 1 g/kg/day, for 5 consecutive days (Wang *et al.*, 2008; Nassar *et al.*, 2017) and G4: ZnO NPs + Se-treated rats. Selenium was given for 8 successive days, 3 of them before the start of the experiment. Rats were sacrificed after the completion of the exposure period.

*Ethical consideration*

The current protocol was reviewed and approved by the guide lines of the Institutional Animal Care and Use Committee (Zagazig University -IACUC) and our approval number is ZU-IACUC/F/109/2020.

*For histopathology*

Skulls were dissected, cerebella were removed, fixed in neutral buffered formalin (10%), and processed for embedding in soft paraffin wax. Sections were de-waxed, hydrated and stained with hematoxylin and eosin (*Bancroft and Gamble, 2008*).

*For electron microscopy (EM)*

Cerebellar specimens were fixed in 3% fresh glutaraldehyde (pH: 7.4), osmicated (buffered 1% OsO<sub>4</sub> at 4°C) and processed till epoxy resin. Ultrathin sections and double staining with uranyl acetate and lead citrate were made (Hayat, 2000). Examination and photographay by a JEOL JEM 2100 electron microscope (Tokyo, Japan) at the Electron Microscopy unit of Faculty of Agriculture, El Mansoura University, Egypt.

*For molecular studies*

Pieces of cerebella were quickly-removed, after sacrifice, from control and experimental groups, preserved in a freezer for Comet assay technic.

*Comet assay*

An accurate single cell gel electrophoresis for detecting and measuring single and double-strand DNA breaks at alkaline medium was performed in the current study according to the methodology of Singh *et al.*(1988) and Tice and Strauss (1995).

## RESULTS

### Characterization of ZnO NPs

Transmission electron microscopic (TEM) description showed that ZnO NPs used in the current study are with tiny and variable sizes ranging from 17.96 to 38.83 nm and good dispersion, allowing easier cellular uptake than NPs of larger sizes. The onset which gives them more surface activity and increased adsorption properties. The TEM image of ZnO nanoparticles prepared by precipitation method showed that particles were spherical grain-like agglomerates with nearly uniform morphology. The mean diameter of particles was 25.3 nm [Fig. 1].

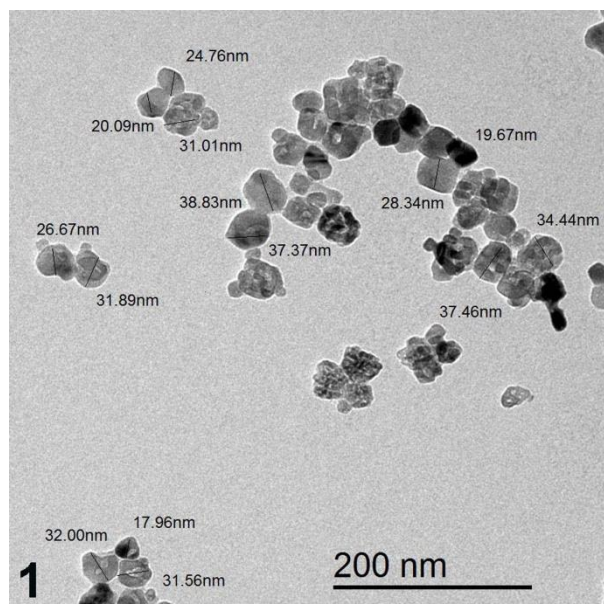
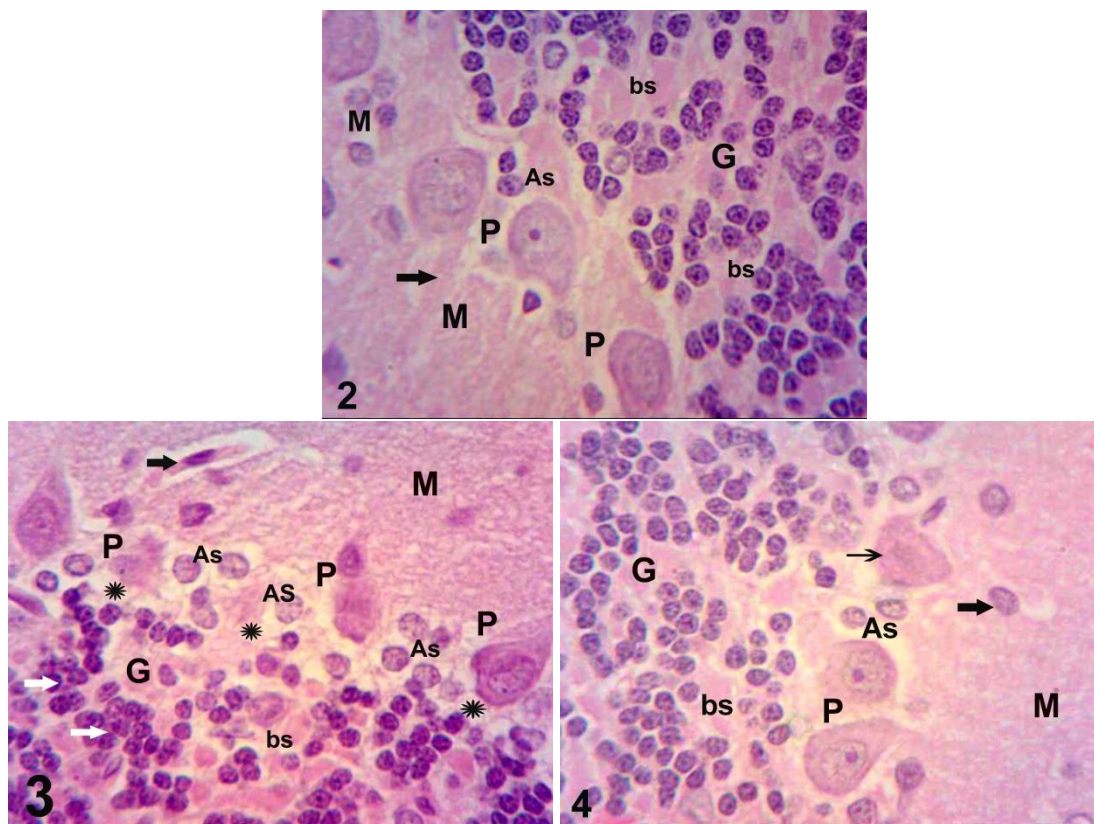


Fig.1: TEM image of ZnO NPs showing the morphology and size. Mean nanoparticle size = 25.3 nm.

### Histopathological results

Examination of H&E-stained sections of control animals illustrated normal histological pattern of cerebellar cortex (Fig. 2). Cerebellum of Se group revealed good histological similarities to that of control. However, exposure of rats to ZnO NPs showed different histopathological lesions in cerebellum. The molecular layer appeared vacuolated with nerve cells possessing darkly-stained nuclei, others are apoptotic and its neuropil was degenerated. Also, a hemorrhage could be detected in the extracellular spaces. Damaged Purkinje cells were surrounded with vacuoles and pericellular spaces and some were lost. Bergman astrocytes appeared swollen. Granular cells appeared degenerated, few in number, necrotic with ill-defined nuclei and mostly overlapped forming gliosis (Fig.3). Co-administration of Se minimized ZnO NPs-induced damage all over the cortical layers to a large extent. Molecular layer appeared normal with intact nerve cells. Purkinje cells appeared in one layer that was similar to control except some damaged cells in the field. Bergmann astrocytes were intact in the vicinity of Purkinje cells exhibiting normal features. Granular cells displayed well-organized pattern, not overlapping each other, with nearly normal blood sinusoids (Fig. 4).



**Fig. 2:** H&E stained sections of cerebellar cortex of control group (x1000) showing small scattered cells of the molecular layer (M), single row of large pyriform cells of Purkinje (P) with pale vesicular nuclei, prominent nucleoli and apparent cellular processes (arrow) passing through molecular layer. Bergman astrocytes (As) are seen around Purkinje cells and granular (G) layer having numerous crowded granular cells with darkly-stained nuclei enclosing blood sinusoids (bs) within their cells. **Fig. 3:** H&E stained sections of cerebellar cortex of ZnONPs group (x1000) showing molecular layer (M) with apoptotic cells (arrow) and vacuolization (v), necrotic Purkinje cells (P) with pericellular spaces (asterisk) and hemorrhage (h), swollen Bergman astrocytes (As). Granular cells (G); numerous, crowded with darkly-stained nuclei in gliosis (white arrow) enclosing blood sinusoids with necrotic cells (n). **Fig. 4:** H&E stained sections of cerebellar cortex of ZnONPs-intoxicated animals treated with Se (x1000) showing restoration of the histological pattern towards the control status, except some affected Purkinje cells.

### Ultrastructural results

Cerebellum of control and selenium groups revealed two types of Purkinje cells (clear and dark) possessing large indented euchromatic nuclei with irregular, visible, double-layered but not dilated nuclear envelope and prominent nucleoli. The clear Purkinje cell having lightly-stained (less electron-dense) cytoplasm. The cytoplasm contains a large number of small electron dense mitochondria of variable sizes and well-organized rough endoplasmic reticulum (rER). Abundant ribosomes were aggregated between the cisternae of rER. The field also exhibited adjacent interstitial microglia cell which appears near the blood capillary (BC) with large nucleus possessing peripheral heterochromatin. The granular cells (GC) exhibiting normal ultrastructural profile closely-packed large spherical nuclei



of granule nerve cells with their characteristic condensed chromatin, their nuclei were surrounded by little cytoplasm (Figs. 5, 6). The molecular layer of cerebellar cortex showed a number of myelinated axons wrapped in a thick myelin sheath with compact arrangement of the myelin lamellae around axons. Another group of non-myelinated axons could be also detected (Fig. 7).

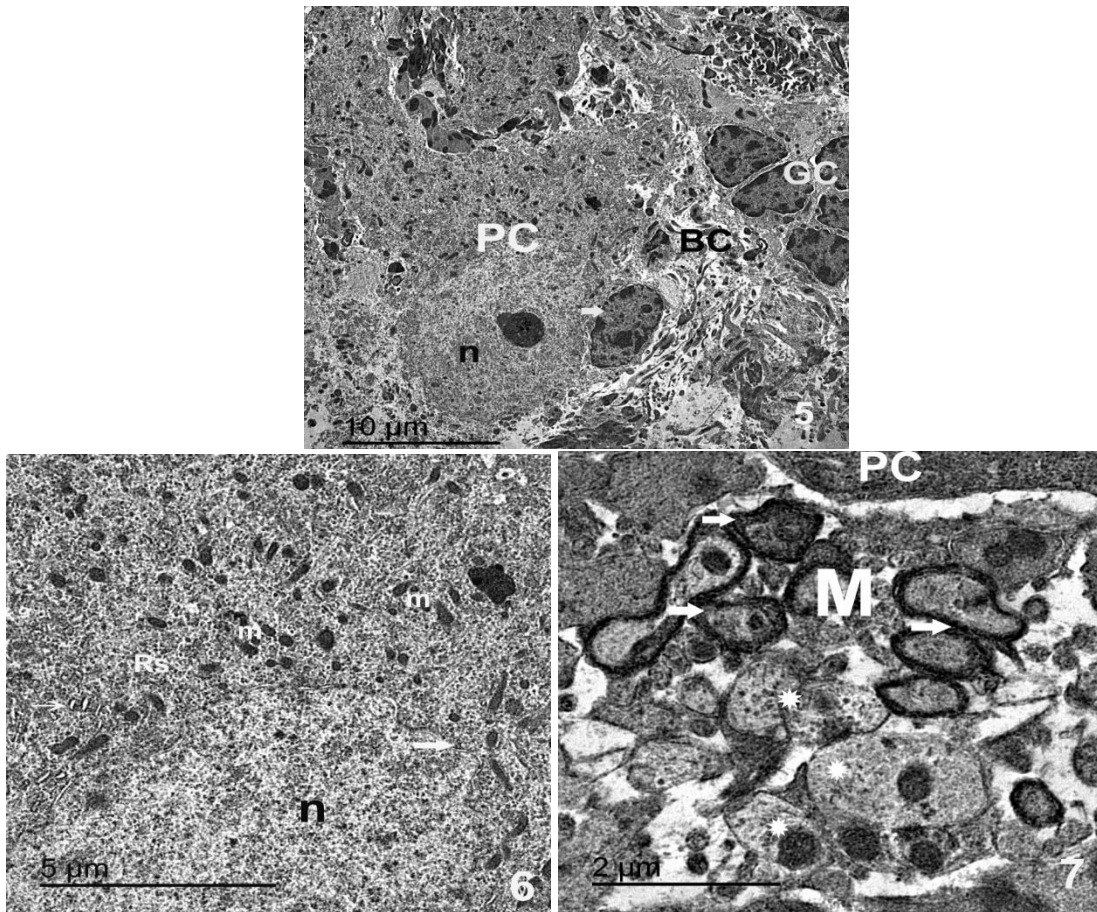


**Fig. 5:** Electron micrograph (EM) of cerebellar cortex of control animal (Scale bar 10μm) showing clear Purkinje cell (PC) having less electron-dense cytoplasm, euchromatic nucleus (n) with well-developed nucleolus. Adjacent interstitial microglia cell (arrow) appears near the blood capillary (BC) with large nucleus possessing margined heterochromatin. A group of granular cells (GC) exhibiting normal ultrastructural profile was evident. **Fig. 6:** Magnified part of the last EM (Scale bar 5μm) illustrating the euchromatic nucleus (n) with irregular, visible but not dilated nuclear envelope (arrow). The cytoplasm contains a large number of small electron dense mitochondria (m) of variable sizes and rER (thin arrow). Abundant ribosomes (Rs) aggregated between the cisternae of rER. **Fig. 7:** EM of cerebellar cortex of control animal (Scale bar 10μm) showing part of the molecular layer (M) adjacent to dark Purkinje cell (PC). A number of myelinated axons (white arrow) are wrapped in a thick myelin sheath with compact arrangement of the myelin lamellae around axons. Another group of non-myelinated axons of the granular cells could be also detected (\*).

Post exposure of animals to ZnONPs cerebellum showed damaged and shrunken PC with heterochromatic nuclei, ill-defined nuclear criteria with complete absence of the nuclear envelop and poor integrity of cell boundary. Cytoplasmic vacuolization was evident. The pericellular spaces appeared due to cellular damage and shrinkage. Also, dilated and ruptured mitochondria could be detected. The field also demonstrates a damaged and shrunken granular cell at the left (Fig.8).

Astrocytes of Bergmann exhibited vacuolated cytoplasm. The field showed an axon hillock emerging from the soma of astrocyte containing damaged mitochondria (Fig. 9). The granular cells had heterochromatic nuclei with irregular nuclear envelopes and some cells showed vacuolated cytoplasm. The myelinated nerve fibers showed dysmyelination in the form of focal areas of splitting of myelin sheath. Vacuolization of neuropil in granular layer was also noticed. The lower part revealed an affected part of the molecular layer illustrating a number of myelinated and demyelinated axons together with affected myelinated nerve fibers with ruptured mitochondria in the axoplasm (Fig. 10).

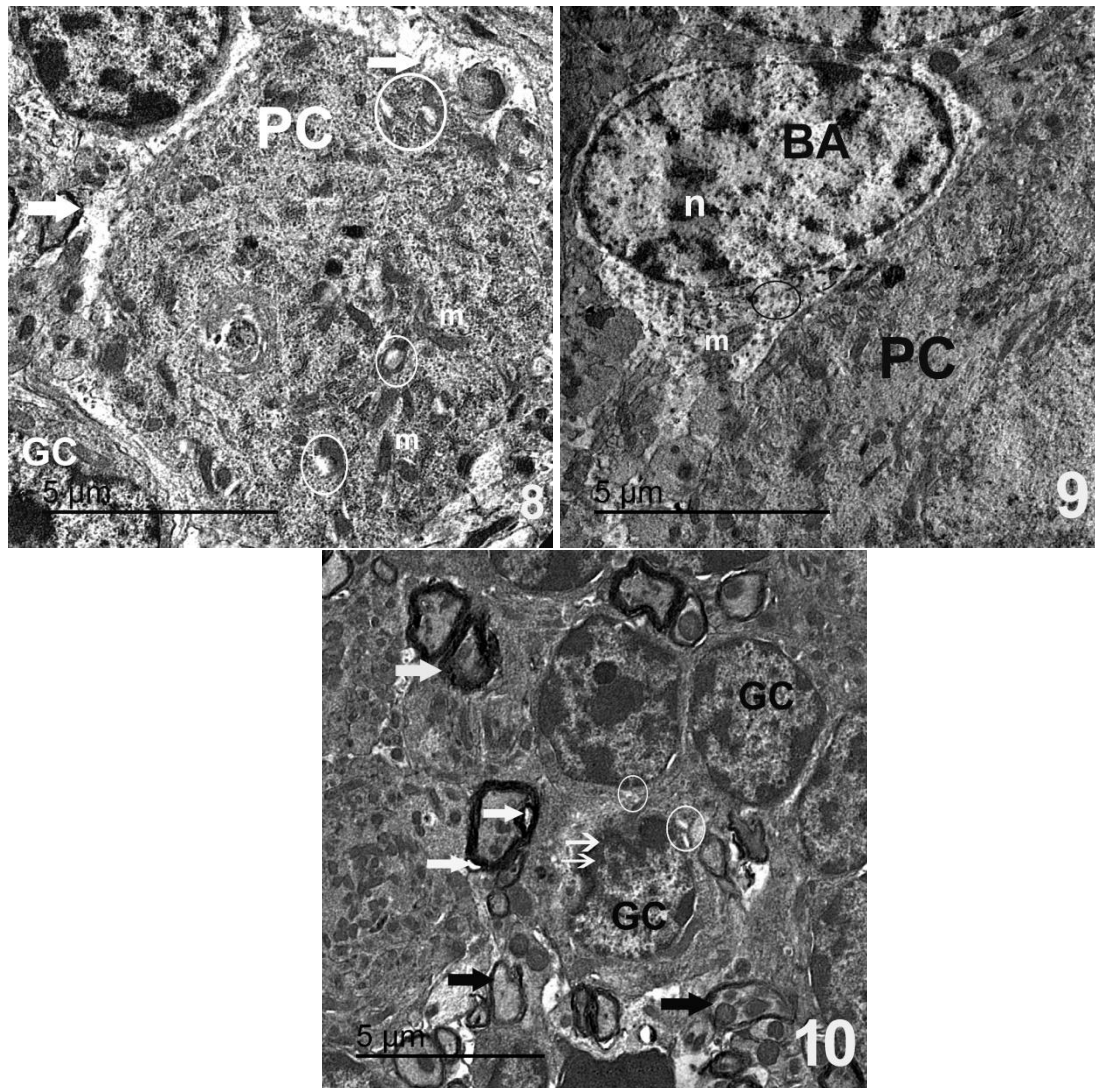


**Fig. 8:** EM of cerebellar cortex of ZnONPs-exposed rat (Scale bar 5 µm) showing a damaged and shrunken PC with relative loss of cell boundary, ill-defined heterochromatic nucleus, with absence of nuclear envelop. Cytoplasmic vacuolization(circles). Pericellular spaces appeared due to cellular damage and shrinkage. Also, dilated and ruptured mitochondria (m) could be detected. The field also demonstrates damaged and shrunken granular cells (GC) at the left. **Fig. 9:** A Bergmann astrocyte exhibited highly vacuolated cytoplasm (circle) and heterochromatic nucleus. The exit of an axon hillock from the soma of astrocyte containing damaged mitochondria (m). **Fig. 10:** showing highly-damaged granular

cells (GC) with heterochromatic nuclei and disrupted nuclear envelope (double arrows) some with vacuolated cytoplasm (circles). Scattered nerve fibers showed dysmyelination (thick white arrows) at certain points. The lower part revealed an affected part of the molecular layer illustrating a number of myelinated and demyelinated axons together with affected myelinated nerve fibers with ruptured mitochondria in the axoplasm (thick black arrows).

Co-administration of Se and ZnO NPs ameliorates the ultrastructural profile of all neural cells of cerebellum. The PC appeared with normal features. It had euchromatic nucleus and intact nuclear membrane. Cytoplasm contains normal mitochondria and lysosomes. Also, the administration of Se improves the ultrastructural pattern of Bergmann astrocytes towards the normal histology to appear with its characteristic heterochromatic nuclei and cytoplasm containing intact mitochondria and intact lysosomes (**Fig. 11**). In other field, cytoplasm appeared possessing euchromatic nuclei with intact nuclear membrane, mitochondria, well organized Golgi and orderly stacks of rER (**Fig. 12**). In the meantime, the cells of the granular series appeared nearly similar to that of control animals with heterochromatic nuclei possessing regular nuclear membranes and homogenous cytoplasm (**Fig. 13**).

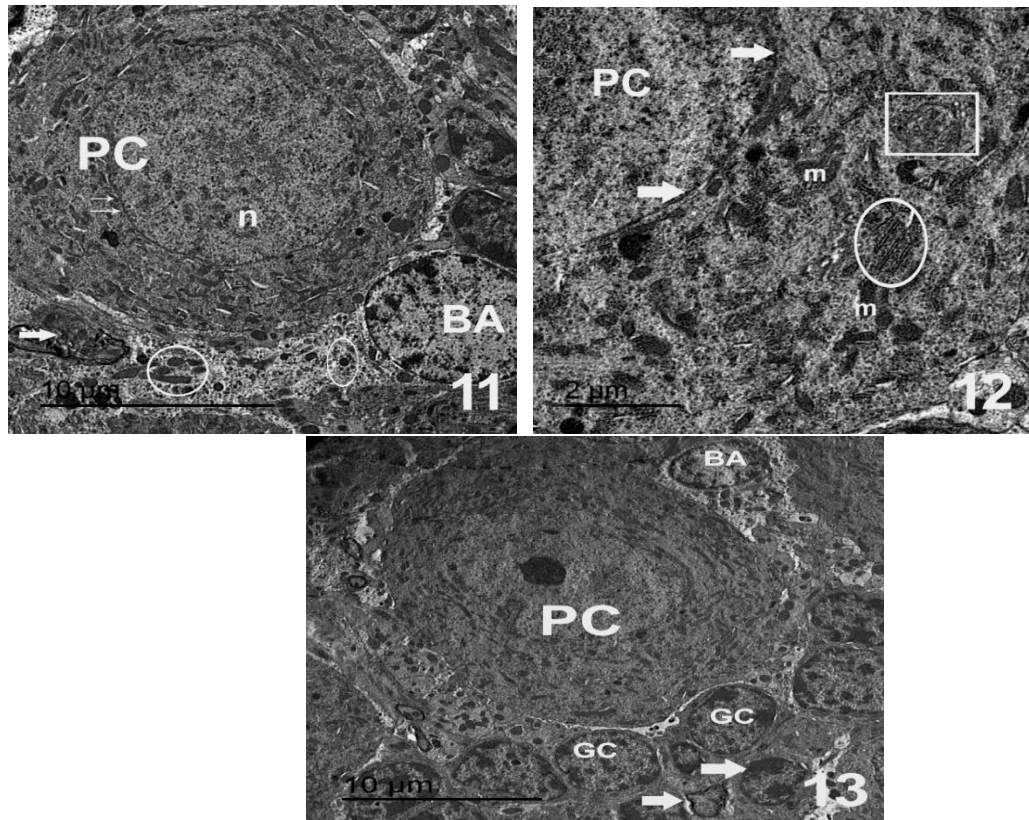


**Fig. 11:** EM of cerebellar cortex of ZnONPs-exposed rat treated with Se (Scale bar 5  $\mu$ m), Purkinje cell (PC) possessing euchromatic nucleus(n) with nuclear intact membrane (double arrows), normal mitochondria (circle) and lysosomes (ovoid), some affected cells (white arrow). Bergman Astrocytes (BA) with normal features. **Fig. 12:** Magnified part (Scale bar 2 $\mu$ m) illustrating a Purkinje cell (PC) with nuclear intact membrane (arrows), most of mitochondria (m) appeared intact, and well organized Golgi (square) and rER in orderly stacks (circle). **Fig. 13:** granular cells (GC) appeared normal with heterochromatic nuclei possessing regular nuclear membranes and homogenous cytoplasm. Normal Purkinje cell (PC) and normal Bergman Astrocyte (BA). Some affected cells (arrows).



# Molecular results:

## DNA fragmentation (Comet assay)

Application of the alkaline comet assay on specimens of cerebellum of control and experimental animals revealed normal DNA fragmentation in control ones with a tail DNA of 0.98% and a tail moment of 1.03. (Fig. 14-1, table 1). Rats administered with Se exhibited a tail DNA and tail moment nearly similar to that of control (1.04% and 0.96 respectively) (Fig. 14-2, table 1). The impact of ZnONPs administration on cerebellar DNA of rat revealed an obvious increase in the tail DNA (2.05%) and tail moment (4.00) (Fig. 14-3, table 1). The synchronized gavage of Se with ZnO to experimental rats protected their cerebella from DNA damage as indicated by a decrease in tail DNA (1.63%) and tail moment (2.59) compared with that of group 3 (Fig. 14-4, table 1).

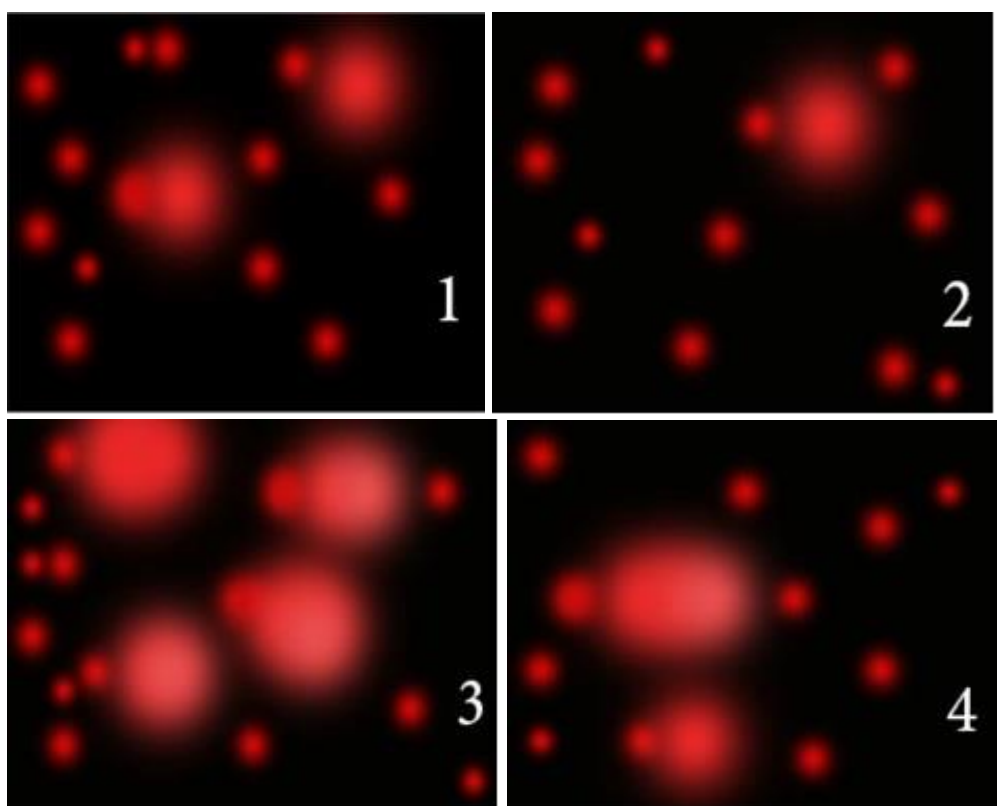


Figure 14(1-4): Gel pictures of comet assay analysis showing the extent of DNA damage in each comet group based on tail DNA% and units of tail moment.

Table 1: values of comet parameters in the control and experimental groups of rats.

	Cerebellum	Tailed	Untailed	Tail length	Tail DNA	Tail Moment
		%	%	μm	%	Unit
NC	1	4	96	1.05	0.98	1.03
Se	2	3	97	0.92	1.04	0.96

ZnO	3	12	88	1.95	2.05	4.00
ZnO + Se	4	8	92	1.59	1.63	2.59

## DISCUSSION

The CNS is highly sensitive to chemical alterations in its microenvironment. Therefore, the entrance of trace amounts of unique materials to brain may change the equilibrium of its internal parenchyma producing damage.

The safety use of ZnO NPs becomes of urgent need due to excessive exposure and miss-manipulation of these nanomaterial in man's environment. Brain and nervous tissues are highly susceptible to oxidative stress-induced damage owing to their high content of unsaturated fatty acids, high exhaustion of oxygen and low levels of antioxidant enzymes (Halliwell, 2006 ; Nazıroğlu, 2009). Our results revealed that, the average size of the ZnO NPs under investigation was 17.96–38.83 nm, and the mean diameter was 25.3 nm measured by the EM since the latter is ideally employed to demonstrate NPs and describe its morphology and size inside tissues. These results are consistent with previous investigators who reported that decreased particle size leads to more ZnO NPs uptake by cells, inducing higher toxicity (Fu *et al.*, 2013; Dkhil *et al.*, 2020). Others recorded that large surface area of ZnO NPs provides more reactivity; which leads to good biological responses obtained in the target living cells (Siddiqi *et al.*, 2018). Moreover, some previous reports confirmed more toxicity of ZnO nano rods and smaller ones than spherical and large ones respectively (Hsiao and Huang, 2011). The unique physicochemical criteria of nanoparticles, especially ZnO NPs, were tightly associated to their biomedical uses (Du *et al.*, 2018; Elshama *et al.*, 2018; Sruthi *et al.*, 2018). Hence, for ZnO NPs; the shape, dose, size and time of exposure should be exactly measured and its toxicity correlated to their physical properties. In the current work, the choice of oral intake of ZnO NPs was because humans have a higher chance of ingestion of them in food-related products and local ointments with varying doses (Sharma *et al.*, 2012). The highest accumulation of NPs, with 18 nm diameter, in the brain was observed after oral gavage (Han *et al.*, 2011; Sawicki *et al.*, 2019)

### Histopathology

The current work recorded histopathological lesions in rat's cerebellum induced by ZnO NPs exposure including; vacuolated molecular layer with apoptotic and degenerated nerve cells. A hemorrhage could be detected in the extracellular spaces. Purkinje cells appeared in more than one layer, sometimes being necrotic and surrounded with pericellular spaces and swollen Bergman astrocytes. The granular cells appeared distorted, necrotic and less in number. Most of them formed gliosis enclosing edematous blood sinusoids. The authors attributed these alterations to the oxidative stress induced by the applied experimental dose of ZnO NPs to extend and confirm its neurotoxicity in a first part of the same study published in (2021) and recorded ZnO NPs toxicity in cerebellum at the immunohistochemical level via up-regulation of caspase-3 and down-regulation of GFAP (Nassar, Salma *et al.*, 2021). The current results are in line with previous findings (Shalaby and Sarhan, 2008;

Sharma *et al.*, 2012; Najafzadeh *et al.*, 2013; Lopes *et al.*, 2014; Ben-Slama *et al.*, 2015; Abbasalipourkabir *et al.*, 2015). Shalaby and Sarhan (2008) recorded a focal loss of Purkinje cells which may be attributed to shrinkage of these cells and withdrawal of their protoplasmic processes following disintegration of cytoskeletal elements. Sharma *et al.* (2012) detected granule cells and Purkinje cells affection (apoptosis, atrophy, decrease in number and degenerated organelles) with different doses and routes of ZnO NPs administration. Abbasalipourkabir *et al.* (2015) recorded a cellular toxicity of ZnONPs (50-200 mg/kg) by increasing the oxidant status and decreasing the antioxidant capacity. These results are in consistent with those of other investigators. The disturbed antioxidant status and apoptotic death in brain cells due to prenatal oral exposure to ZnO NPs was recorded in rats. These NPs damaged hippocampus and cerebral cortex and induced reactional changes which stop memory and learning (Xiaoli *et al* 2017). NPs may enhance neurodegenerative diseases by allowing release of ROS, inflammation, microglial activation and focal loss of neurons (Wang *et al.*, 2017). Abdel-Aziz *et al.* (2018) concluded that, rats exposed to ZnO NPs disturbed normal linear organization of Purkinje cells in the form of multilayer pattern which explained as an adaptive response to neuronal injury in a trail to re-construct good synapses with neighboring nerve cells in order to perform their function. In addition, Amer and Karam (2018) recorded similar histopathological changes, whorled masses of axons and gliosis in cerebellum of ZnO NPs-exposed animals and attributed gliosis to reactive proliferation of astrocytes in GFAP immune-stained sections. Apoptosis and necrosis were also recorded with ZnO NPs – exposure in the same organ (Elmore, 2007) or in different organs (Wells *et al.*, 2012; Nassar *et al.*, 2017). Zinc NPs caused peri-neural vacuolization, congested vascularity in brain tissue as compared to control (Dkhil *et al.*, 2020).

#### *Electron microscopy*

The ultrastructural changes in all neuronal cells of cerebellum, recorded in the current study, as affected by ZnONPs are in parallel with those of previous investigations. Elshama *et al.*, (2017) reported that ZnO NPs caused considerable damage to the cytoplasmic organelles concerned with the biosynthesis of cell proteins. Elshama *et al.* (2018) found that prolonged exposure to Zn NPs induced ultrastructural alterations brain of rats, based on dosage and ROS production. Cytoplasmic vacuolization in Bergmann astrocytes was recorded as a pathological response to various stimuli (Guillamón-Vivancoset *et al.*, 2015). Rafati *et al.* (2015) reported that degeneration of Bergmann astrocytes led to concomitant degeneration of Purkinje cells. Thus, degeneration of the first ones might explain the degeneration and loss of the second. The granular neurons exhibited heterochromatic nuclei with irregular nuclear membranes and vacuolated cytoplasm due to oxidative stress (Kamal and Kamal, 2013; D'Angelo *et al.*, 2013). Costa *et al.* (2014) suggested that granular cells changes were correlated to alterations occurred in Purkinje neurons leading to gradual loss of harmony between both types of neurons. The vacuolization of neuropil might be attributed to shrinkage of cells and withdrawal of their processes after cytoskeletal affection as a sign of neuronal death. Ultrathin section examination revealed axonal changes in the form of dysmyelination in addition to vacuolar changes of axoplasm and occurrence of demyelination (Afifi and Embaby, 2016). Dusart *et al.* (2006) described Purkinje cell's degeneration which began in cell bodies with rough ER alterations and polysomal

aggregation. Then, shrinkage of cytoplasm and chromatin condensation occur suggesting cell death. Moreover, Fu *et al.* (2013) recorded localization of NPs as electron dense granules between myelin lamellae of cerebellar nerve fibers of exposed animals. Abdel-aziz *et al.* (2018) demonstrated shrunken Purkinje cells with condensed nuclei, vacuolated cytoplasm and fragmented Golgi apparatus (in rats received 50 mg / kg ZnO NPs). Also, Bergmann astrocytes, granule cells and myelinated nerve fibers were affected. But when rats received 200 mg/kg ZnONPs all the neural cells appeared more affected.

#### *DNA damage*

Concerning the impact of ZnO NPs exposure on cerebellar tissue at the molecular level, in the present investigation, Comet technology was used. The technic verifies two goals; detection of DNA damage at an early stage and giving a positive response at a lower concentration. Therefore, the present results proved that ZnO NPs-induced DNA injury in rat's cerebellum at the dose level of 1g/kg /day as recorded from comet data. However, supplementation with Se (0.2 mg/kg b.w. / day) minimized this harmful effect towards the normal status. The increase in tail length of DNA at the used dose may reflect a high percent of DNA strand break. The authors correlated this genotoxicity to the oxidative (ROS liberation) and nitrosative effects induced by ZnO NPs. The inflammatory cytokines release could also contribute to DNA injury caused by ZnO NPs (Totsuka *et al.*, 2014). The role of Se at this situation provides additional evidence to its possible protective potential at the molecular level. These findings confirm the neurotoxicity of ZnO NPs at the level of DNA and being in line with previous investigators (Tian *et al.*, 2015; Attia *et al.*, 2018; Dkhil *et al.*, 2020). Tian *et al.* (2015) reported that Zn NPs exposure *in vitro* caused DNA damage in mice brain cell lines. Attia *et al.* (2018) showed that Zn NPs exposure (at two different concentrations) for one week induced brain DNA fragmentation (*in vivo* study). The authors explained the DNA damage as a result of oxidative stress due to Zn NPs gavage. Also, ZnO NPs exposure caused statistically-significant DNA damage and increased chromosomal aberrations (Dufour *et al.*, 2006; Sharma *et al.*, 2009). Oxidative stress occurred even when only small amounts of ZnO NPs were combined into cells. This led to accumulation of ROS that attack DNA, releasing a huge range of base and sugar modifications and a number of alterations such as DNA cleavage and oxidation of purines. Induction of ROS can occur spontaneously once ZnO NPs are exposed to the acidic medium of lysosomes owing to their chemical and surface nano-level characteristics. These interactions disturb the ability of biological system to expel the toxic metabolites or to repair the resulting damage (Ansar *et al.*, 2017). Moreover, the damaging effect of ZnO-NPs on DNA was investigated in the testicular tissue by Nassar *et al.* (2017) using Comet assay. The authors recorded a significant increase in the tail length, DNA % in the tail and tail-DNA moment in testis of rats. Previous studies suggested that ZnO-induced DNA damage may be correlated to oxidative stress and lipid peroxidation (Xiong *et al.*, 2011). The released ROS react directly with DNA, causing damage to both pyrimidine and purine bases as well as the DNA backbone (Martinez *et al.*, 2003). Nassar *et al.* (2018) concluded that TiO<sub>2</sub>-NPs induces oxidative stress, which produces cytotoxic changes in sperms and increased the apoptotic index in these germ cells via the increased expression of caspase 3 which may affect the fertilizing potential of spermatozoa and vitamin E minimizes this toxicity. Previous studies recorded that after exposure to 15 µg/mL

Nano-ZnO particles for 3 hours, reduced the activity of mouse neural stem cells, DNA damage and cell apoptosis was reported (Deng *et al.*, 2009).

### *Selenium*

Regarding the gradual exposure to zinc oxide nanoparticles and their certain neurodegenerative and cytotoxic effects, in the present study, compounds with antioxidant and anti-inflammatory functions may constitute promising protective and/or therapeutic policies to overcome neurotoxicity induced by ZnO NPs. Supplementation of selenium to ZnO NPs-intoxicated rats, in the existing study, minimized the damage resulted from ZnO NPs all over the parenchyma of the cerebellar cortex to a large extent. Molecular layer appeared normal with intact nerve cells. Purkinje cells of this group displayed an aligned layer. Bergmann astrocytes exhibited normal features. Granular cells displayed well-organized pattern, not overlapping each other with nearly normal blood sinusoids. In the meantime, the combination of Se and ZnO NPs partially-protect the ultrastructural and molecular profiles of the neural cells in cerebellum, the onset which maximizes the role of Se as an antioxidant and/or neuroprotective material at the cellular, subcellular and molecular levels. These findings are in agreement with those of previous investigators; where Smith *et al*, 2010 reported that Selenium (Se) is an important nutritive substance for the servicing of human health, which plays a worthy role in reducing oxidative stress in the brain. Se in vivo is primarily present as various selenoproteins that preserve the balance of the cellular redox state. Also, supplementation with Se reduces lipid peroxidation and DNA damage induced by Hg exposure Li *et al*, 2012. Further, selenium methionine protects from neuronal degeneration induced by MeHg exposure in rats Sakamoto *et al*, 2013. Selenium is a compound previously used for antioxidant purposes in animal models of experimentally-induced nephrotoxicity Wan *et al*, 2017 and Gunes *et al*, 2018. Various studies recorded selenoproteins to play an important role in antioxidant defense systems in myocardium Soudani *et al*, 2011, and Se has anti-inflammatory El-Ghazaly *et al*, 2016 and Tyszka-Czochara *et al*, 2016 and antiapoptotic effects Balaban *et al*, 2017, Jin *et al*, 2017 and Demirci *et al*, 2017. Tu *et al*, 2021 reported that, treatment of rats with selenium, remarkably- improved organizations, structures and swelling of membranous organelles of cerebellum towards the normal features after MeHg exposure. Geraniol (an antioxidant) improved memory decay and neurotoxicity induced by ZnO NPs in male rats Farokhchah *et al*, 2021. In conclusion, our results extend and confirm the neurotoxicity of ZnO NPs at the cellular, subcellular and molecular levels and suggest Se as a supplement with a promising neuro-protective role against toxicity of ZnO NPs.

### References:

1. Abbasalipourkabir R, Moradi H, Zarei S, Asadi S, Salehzadeh A, Ghafourikhosroshahi A, Mortazavi M and Ziamajidi N (2015). Toxicity of zinc oxide nanoparticles on adult male Wistar rats. *Food Chem Toxicol*, 84: 154-160.



2. Abdel-Aziz HM, Mekawy NH and Ibrahim NE (2018). Histological and immunohistochemical study on the effect of zinc oxide nanoparticles on cerebellar cortex of adult male albino rats. *The Egypt J Histol.*, 42(1): 23-34.
3. Afifi OK and Embaby AS (2016). Histological study on the protective role of ascorbic acid on cadmium induced cerebral cortical neurotoxicity in adult male albino rats. *J Microsc Ultrastr.*, 4(1): 36-45.
4. Al-Salmi FA, Hamza RZ and El-Shenawy NS (2019). The interaction of zinc oxide/green tea extract complex nanoparticles and MSG in liver of rats. *Current Pharmaceutical Biotechnology*, 20(6): 465-475.
5. Amer MG and Karam RA (2018). Morphological and Biochemical Features of Cerebellar Cortex after Exposure to Zinc Oxide Nanoparticles: Possible Protective Role of Curcumin. *The Anatomical Record*, 30: 1454-1466.
6. and brain of aged rats with scopolamine-induced dementia. *Metab*
7. Ansar S, Abudawood M, Hamed SS and Aleem MM (2017). Exposure to zinc oxide nanoparticles induces neurotoxicity and proinflammatory response: amelioration by hesperidin. *Bio Trace Elem Res*, 175(2): 360-366.
8. attenuates apoptosis, inflammation and oxidative stress in the blood
9. Attia H, Nounou H and Shalaby M (2018). Zinc Oxide Nanoparticles Induced Oxidative DNA Damage, Inflammation and Apoptosis in Rat's Brain after Oral Exposure. *Toxics*, 6(2): 29-49.
10. Balaban H, Nazıroğlu M, Demirci K and Övey İS (2017). The protective
11. Bancroft JD and Gamble M (2008). *Theory and Practice of Histological Techniques*, 6th ed. Elsevier Churchill Livingstone: Philadelphia, PA, USA; pp. 601-641.
12. Ben-Slama I, Mrad I, Rihane N, EL Mir L, Sakly M and Amara S (2015). Sub-acute oral toxicity of zinc oxide nanoparticles in male rats. *J Nanomed Nanotechnol*, 6(3): 284-290.
13. *Brain Dis*, 32(2): 321-329.
14. Costa LG, Cole TB, Coburn J, Chang YC, Dao K and Roque P (2014). Neurotoxicants are in the air: convergence of human, animal, and in vitro studies on the effects of air pollution on the brain. *Bio Med Res Int*, 1-8.
15. D'Angelo E, Solinas S, Mapelli J, Gandolfi D, Mapelli L and Prestori F (2013). The cerebellar Golgi cell and spatiotemporal organization of granular layer activity. *Front neural circuits*, 7: 93-113.
16. Demirci K, Nazıroğlu M, Övey İS and Balaban H (2017). Selenium
17. Deng XY, Luan QX, Chen WT and Wang YL (2009). Nanosized zinc oxide particles induce neural stem cell apoptosis. *Nanotechnology* 20(11): 115101-115107.
18. Dkhil MA, Diab MS, Aljawdah HM, Murshed M, Hafiz TA, Al-Quraishy S and Bauomy A (2020). Neuro-biochemical changes induced by zinc oxide nanoparticles. *Saudi Journal of Biological Sciences*, 27: 2863-2867.

19. Du LJ, Xiang K, Liu JH, Song ZM, Liua Y, Cao A and Wang H (2018). Intestinal injury alters tissue distribution and toxicity of ZnO nanoparticles in mice. *Toxicol.Lett*, 295: 74-85.
20. Dufour EK, Kumaravel T, Nohynek GJ, Kirkland D and Toutain H (2006). Clastogenicity, photo-clastogenicity or pseudo-photo-clastogenicity: genotoxic effect of zinc oxide in the dark, in pre-irradiated or simultaneously irradiated Chinese hamster ovary cells. *Mutat Res*, 607: 215-224.
21. Dusart I, Guenet J L and Sotelo C (2006). Purkinje cell death: Differences between developmental cell death and neurodegenerative death in mutant mice. *Cerebellum*, 5: 163-173.
22. El-Demerdasha Fatma M. and Nasr Hoda M (2014). Antioxidant effect of selenium on lipid peroxidation, hyperlipidemia and biochemical parameters in rats exposed to diazinon. *Journal of Trace Elements in Medicine and Biology*, 28: 89-93.
23. El-Ghazaly MA, Fadel N, Rashed E, El-Batal A and Kenawy SA (2016). Anti-inflammatory effect of selenium nanoparticles on the inflammation induced in irradiated rats. *Can J Physiol Pharmacol*, 95(2): 101-110.
24. Elmore S (2007): Apoptosis: a review of programmed cell death. *Toxicologic pathology*, 35(4): 495-516.
25. Elshama SS, Abdallah ME and Abdel-Karim RI (2018). Zinc Oxide Nanoparticles: Therapeutic Benefits and Toxicological Hazards. *Nanomed J*, 5: 16-22.
26. Elshama SS, Aly SM, Abdalla ME and Hassan WA (2017). Postmortem identification of spermatozoa on human skin based on fluorescent monoclonal antibody method. *Archiwum Medycyny Sądowej i Kryminologii/Archives of Forensic Medicine and Criminology*, 67(2): 121-133.
27. Farokhcheh M, Hejzian L, Akbarnejad Z, Pourabdolhossein F, Hosseini SM, Mehraei TM and Soltanpour N (2021). Geraniol improved memory impairment and neurotoxicity induced by zinc oxide nanoparticles in male wistar rats through its antioxidant effect. *Life Sciences*, 282: 119823.
28. Feng XL, Chen AJ, Zhang YL, Wang JF, Shao LQ and Wei LM (2015). Central nervous system toxicity of metallic nanoparticles. *Int J Nanomed*, 10: 4321-4340.
29. Fu C, Liu T, Li L, Liu H, Chen D and Tang F (2013). The absorption, distribution, excretion and toxicity of mesoporous silica nanoparticles in mice following different exposure routes. *Biomaterials*, 34: 2565-2575.
30. Guillamón-Vivancos T, Gómez-Pinedo U and Matías-Guiu J (2015). Astrocytes in neurodegenerative diseases (I): function and molecular description. *Neurol (Engl Ed)*, 30(2): 119-129.
31. Gunes S, Sahinturk V, Uslu S, Ayhanci A, Kacar S and Uyar R (2018). Protective effects of selenium on cyclophosphamide-induced oxidative stress and kidney injury. *Biol Trace Elem Res*, 185(1): 116-123.
32. Halliwell B (2006). Oxidative stress and neurodegeneration, where are we now? *J Neurochem*, 97(6): 1634-1658.

33. Han D, Tian Y, Zhang T, Ren G and Yang Z (2011). Nano-zinc oxide damages spatial cognition capability via over-enhanced long-term potentiation in hippocampus of Wistar rats. *Int J Nanomed*, 6: 1453-1461.
34. Hayat MA (2000). *Principles and Techniques of Electron Microscopy: Biological Applications*. Cambridge: Cambridge Univ Press, 546-558.
35. Hsiao I and Huang Y (2011). Effects of various physiochemical characteristics on the toxicities of ZnO and TiO<sub>2</sub> nanoparticles toward human lung epithelial cell. *Sci Total Environ*, 409(7): 1219-1228.
36. Jachak A, Lai S, Hida K, Suk J, Markovic N, Biswal S, Breysse P and Hanes J (2012). Transport of metal oxide nanoparticles and single-walled carbon nanotubes in human mucus. *Nanotoxicology*, 6: 614-622.
37. Jin X, Xu Z, Zhao X, Chen M and Xu S (2017). The antagonistic effect
38. Kamal I and Kamal H (2013). Effects of aluminum on rat cerebellar cortex and the possible protective role of *Nigella sativa*: a light and electron microscopic study. *The Egypt J Histol*, 36: 979-990.
39. Li CH, Shen C, Cheng Y, Huang S, Wu C, Kao C, Liao J and Kang J (2012). Organ distribution, clearance and genotoxicity of oral administered zinc oxide nanoparticles in mice. *Nanotoxicology*, 6(7): 746-756.
40. Li YF, Dong ZQ, Chen CY, Li B, Gao YX, Qu LY, Wang TC, Fu X, Zhao YL and Chai ZF (2012). Organic selenium supplementation increases mercury excretion and decreases oxidative damage in long-term mercury-exposed residents from Wanshan, China. *Environ. Sci. Technol.*, 46, 11313-11318.
41. Lopes S, Ribeiro F, Wojnarowicz J, Łojkowski W, Jurkschat K, Crossley A, Soares AMVM and Loureiro S (2014). Zinc oxide nanoparticles toxicity to *Daphnia magna*: Size-dependent effects and dissolution. *Environ Toxicol Chem*, 33: 190-198.
42. Martinez GR, Loureiro AP, Marques SA, Miyamoto S, Yamaguchi LF, Onuk J, Almeida EA, Garcia CC, Barbosa LF, Medeiros MH and Di M (2003). Oxidative and alkylating damage in DNA. *Mutat Res*, 544: 115-127.
43. Najafzadeh H, Ghoreishi S M, Mohammadian B, Rahimi E, Afzalzadeh M R, Kazemivarnamkhasti M and Ganjealidarani H (2013). Serum biochemical and histopathological changes in liver and kidney in lambs after Zinc Oxide nanoparticles administration. *Vet World*, 6: 534-537.
44. Nassar SA, Ghonemy OI, Awwad MH, Mahmoud MS and Alsagati YM (2017). Cyto and Genotoxic Effects of Zinc Oxide Nanoparticles on Testicular Tissue of Albino Rat and the Protective Role of Vitamin E. *Transylvanian Review*, 25(22): 5809-5819.
45. Nassar SA, Zayed FAB, Salama MA and Tabatabaee SBM (2018). Histological and Molecular Studies on the Toxicity of Titanium Dioxide Nanoparticles in Testis and Bone Marrow of Albino Mice. *World Applied Sciences Journal*, 36(3): 562-571.

46. Nassar Salma S, Salama ES and Abd El-Gawad AM (2021). Selenium Protects Caspase 3 and Glial Fibrillar Acidic Protein (GFAP) Expression in Cerebellum of Rats against Zinc Oxid Nanoparticles (Znonps) Exposure. *Annals of the Romanian Society for Cell Biology*, 25(6): 08-23.
47. Nazıroğlu M (2009). Role of selenium on calcium signaling and oxidative stress- induced molecular pathways in epilepsy. *Neurochem Res*, 34: 2181-2191.
48. of selenium on lead-induced apoptosis via mitochondrial dynamics
49. pathway in the chicken kidney. *Chemosphere*, 180: 259-266.
50. Pati R, Das I, Mehta RK, Sahu R and Sonawane A (2016). Zinc-oxide nanoparticles exhibit genotoxic, clastogenic, cytotoxic and actin depolymerization effects by inducing oxidative stress responses in macrophages and adult mice. *ToxicolSci*, 150(2): 454-472.
51. Rafati A, Erfanizadeh M, Noorafshan A and Karbalay- Doust S (2015). Effect of benzene on the cerebellar structure and behavioral characteristics in rats. *Asian Pac J Tropi Biomed*, 5(7): 568-573.
52. Ransohoff RM (2016). How neuro-inflammation contributes to neuro-degeneration. *Science*, 353(6301): 777-783.
53. role of selenium on scopolamine-induced memory impairment, oxidative stress, and apoptosis in aged rats: the involvement of TRPM2 and TRPV1 channels. *Mol Neurobiol*, 54(4): 2852-2868.
54. Sakamoto M, Yasutake A, Kakita A, Ryufuku M, Chan HM, Yamamoto M, Oumi S, Kobayashi S and Watanabe C (2013). Selenomethionine protects against neuronal degeneration by methylmercury in the developing rat cerebrum. *Environ. Sci. Technol.*, 47: 2862-2868.
55. Sawicki K, Czajka M, Matysiak-Kucharek M, Fal B, Drop B, Me,czyn' ska-Wielgosz S, Sikorska K, Kruszewski M and Kapka-Skrzypczak L (2019). Toxicity of metallic nanoparticles in the central nervous system. *Nanotechnol Rev*, 8: 175-200.
56. Shalaby NM and Sarhan NI (2008). Light and electron microscopic study on the effect of valproic acid on cerebellar cortex of adult male albino rats and the possible protective effect of l-carnitine. *Egypt J Histo*, 256-265.
57. Sharma V, Anderson D and Dhawan A (2011). Zinc oxide nanoparticles induce oxidative stress and genotoxicity in human liver cells (HepG2). *J Biomed Nanotechnol*. 7(1): 98-99.
58. Sharma V, Anderson D and Dhawan A (2012). Zinc oxide nanoparticles induce oxidative DNA damage and ROS-triggered mitochondria mediated apoptosis in human liver cells (HepG2). *Apoptosis*, 17: 852-870.
59. Sharma V, Shukla RK, Saxena N, Parmar D, Das M, and Dhawan A (2009). DNA damaging potential of zinc oxide nanoparticles in human epidermal cells. *Toxicology Letters*, 185: 211-218.
60. Shim KH, Hulme J, Maeng EH, Kim MK and An SS (2014). Analysis of zinc oxide nanoparticles binding proteins in rat blood and brain homogenate. *Int J Nanomed*, 15: 217-224.
61. Siddiqi KS, urRahman A, Tajuddin SM and Husen A (2018). Properties of zinc oxide nanoparticles and their activity against microbes. *Nanoscale Res Lett*, 13(1): 1-13.

62. Singh NP, McCoy MT, Tice RR and Schneider EL (1988). A simple technique for quantitation of low levels of DNA damage in individual cells. *Experimental cell research*, 175(1): 184-191.
63. Smith A, Giunta B, Bickford P C, Fountain M, Tan J and Shytle R D (2010). Nanolipidic particles improve the bioavailability and  $\alpha$ -secretase inducing ability of epigallocatechin-3-gallate (EGCG) for the treatment of Alzheimer's disease. *International journal of pharmaceuticals*, 389(1-2): 207-212.
64. Soudani N, Troudi A, Bouaziz H, Ben Amara I, Boudawara T and Zeghal N (2011). Cardioprotective effects of selenium on chromium (VI)-induced toxicity in female rats. *Ecotoxicol Environ Saf*, 74: 513-520.
65. Sruthi S, Ashtami J and Mohanan PV (2018). Biomedical application and hidden toxicity of Zinc oxide nanoparticles. *Mater Today Chem*, 10: 175-186.
66. Tian L, Lin B, Lei W L, Li K, Liu H and Xi Z (2015). Neurotoxicity induced by zinc oxide nanoparticles: age-related differences and interaction. *Sci Rep*, 5(1): 1-12.
67. Tice RR and Strauss GHS (1995). The single cell gel electrophoresis comet assay - a potential tool for detecting radiation-induced DNA damage in humans. *Stem Cells*, 13(1): 207-214.
68. Totsuka Y, Ishino K, Kato T, Goto S, Tada Y, Nakae D, Watanabe M and Wakabayashi K (2014). Magnetite nanoparticles induce genotoxicity in the lungs of mice via inflammatory response. *Nanomaterials*, 4: 175-188.
69. Tu R, Zhang C, Feng L, Wang H, Wang W and Li P (2021). Impact of selenium on cerebellar injury and mRNA expression in offspring of rat exposed to methylmercury. *Ecotoxicology and Environmental Safety*, 223: 112584.
70. Tyszk-Czochara M, Pasko P, Zagrodzki P, Gajdzik E, Wietecha-Posluszny R and Gorinstein S (2016). Selenium supplementation of amaranth sprouts influences betacyanin content and improves anti-inflammatory properties via NF $\kappa$ B in murine RAW264.7 macrophages. *Biol Trace Elem Res*, 169(2): 320-330.
71. Wan H, Zhu Y, Chen P, Wang Y, Hao P, Cheng Z, Liu Y and Liu J (2017). Effect of various selenium doses on chromium (IV)-induced nephrotoxicity in a male chicken model. *Chemosphere*, 174: 306-314.
72. Wang B, Feng W, Wang M, Wang T, Gu Y, Zhu M, Ouyang H, Shi J, Zhang F, Zhao Y and Chai Z (2008). Acute toxicological impact of nano-and submicro-scaled zinc oxide powder on healthy adult mice. *Journal of Nanoparticle Research*, 10(2): 263-276.
73. Wang Y, Xiong L and Tang M (2017). Toxicity of inhaled particulate matter on the central nervous system: neuroinflammation, neuropsychological effects and neurodegenerative disease. *J Appl Toxicol*, 37(6): 644-667.
74. Wells M A, Abid A, Kennedy I M and Barakat A I (2012). Serum proteins prevent aggregation of Fe<sub>2</sub>O<sub>3</sub> and ZnO nanoparticles. *Nanotoxicology*, 6: 837-846.



75. Xiaoli F, Junrong W, Xuan L, Yanli Z, Limin W, Jia L and Longqua S (2017). Prenatal exposure to nano sized zinc oxide in rats: Neurotoxicity and postnatal impaired learning and memory ability. *Nanomedicine*, 12: 777-795.
76. Xiong D, Fang T, Yu L, Sima X and Zhu W (2011). Effects of Nano-scale TiO<sub>2</sub>, ZnO and their bulk counterparts on zebra fish: Acute toxicity, oxidative stress and oxidative damage. *Sci Total Environ*, 409(8): 1444-1452.
77. Yuan J, Chen Y, Zha H, Song L, Li C Y L and Xia X (2010). Determination, characterization and cytotoxicity on HELF cells of ZnO nanoparticles. *Colloids Surf B Biointerfaces*, 76(1): 145-150.
78. Zanchi MM, Vanusa M, Daniela DB, Laura MV, Cristiano CS, Melina BS, Aryele PI and Francielli WS (2015). Green tea infusion improves cyclophosphamide-induced damage on male mice reproductive system. *Toxicology Reports*, 2: 252-260.